Tomographic retrieval of the polarization state of an ultrafast laser pulse

Philip Schlup,[1,*] Omid Masihzadeh,[1] Lina Xu,[2] Rick Trebino,[2] and Randy A. Bartels[1]

[1]*Department of Electrical and Computer Engineering, Colorado State University, Fort Collins, Colorado 80523, USA*
[2]*School of Physics, Georgia Institute of Technology, Atlanta, Georgia 30332, USA*
*Corresponding author: philip.schlup@colostate.edu

We introduce a self-referenced method for determining the complete polarization state of an ultrafast pulse field. The algorithm is based on any well-established technique that measures both the intensity and phase of a single polarization, such as frequency-resolved optical gating (FROG). We demonstrate the retrieval of nontrivial fields generated using a polarization-amplitude-phase ultrafast pulse shaper using four standard FROG measurements. © 2008 Optical Society of America

OCIS codes: 260.5430, 320.5540, 260.7120.

The response of many physical systems to illumination by a femtosecond laser pulse is significantly impacted by the polarization state of that pulse [1–3]. This has stimulated interest in extending the development of ultrafast pulse shaping technology [4] to the control of ultrafast polarization [5–8]. These pulse shapers have been successfully implemented for optimization of polarization-dependent ionization [1,2], correction of polarization distortion in fiber propagation [9], and coherent anti-Stokes Raman microscopy [7]. However, few techniques have been reported for characterizing the polarization state of ultrashort pulses. One method, termed POLLIWOG [10], uses spectral interferometry to characterize two orthogonal polarization components relative to a well-characterized reference pulse. The polarization dependence of self- and cross-phase modulation have also been adapted for polarization measurement [11,12].

In this Letter, we introduce a self-referenced technique for fully characterizing the polarization state of an arbitrary ultrashort pulse. Our technique, which we call the tomographic ultrafast retrieval of transverse light E-fields (TURTLE), establishes the full polarization state using three measurements of the pulse at different angular orientations of a polarizer in a manner related to the Stokes parameters [13]. We investigate two versions of the retrieval algorithm. In the first, we find an analytical expression for combining three complex fields with known angles and relative amplitudes; the second employs a search algorithm to fit to four measured frequency-resolved optical gating (FROG) traces.

We write the field for an arbitrary polarization-shaped pulse in the frequency domain as $\widetilde{\mathbf{E}}(\Omega) = \widetilde{E}_x(\Omega)\hat{\mathbf{x}} + r\widetilde{E}_y(\Omega)e^{-i(\Omega\tau+\theta)}\hat{\mathbf{y}}$, where $\Omega = \omega - \omega_0$, for a central frequency ω_0, and $\widetilde{E}_x(\Omega)$ and $\widetilde{E}_y(\Omega)$ represent the complex spectra along $\hat{\mathbf{x}}$ and $\hat{\mathbf{y}}$ spatial coordinate directions, respectively. Using a polarizer at various angles η relative to the $\hat{\mathbf{x}}$ axis to isolate projections of $\widetilde{\mathbf{E}}(\Omega)$, we measure $\widetilde{E}_x(\Omega)$ and $\widetilde{E}_y(\Omega)$. The relative am-

plitude coefficient r can be determined experimentally through independent power measurements P of each polarization projection, which are easily performed in most experiments. Normalizing the reconstructed fields such that $\int |\widetilde{E}_\eta(\Omega)|^2 d\Omega = 1$, it is directly given by $r = (P_y/P_x)^{1/2}$.

To establish the full polarization state, we must determine the relative time delay τ, and the relative phase θ, between the $\hat{\mathbf{x}}$ and $\hat{\mathbf{y}}$ components. Since self-referenced amplitude and phase measurements of a single pulse are insensitive to the arrival time and absolute phase, this necessitates at least one additional measurement at an angle $\eta \neq \{0, 90°\}$. This will take the form $r_\eta \widetilde{E}_\eta(\Omega)e^{-i(\Omega\tau_\eta+\theta_\eta)} = \cos\eta\,\widetilde{E}_x(\Omega) + r\sin\eta\,\widetilde{E}_y(\Omega)e^{-i(\Omega\tau+\theta)}$, where τ_η and θ_η account for, respectively, the delay and phase of the η measurement relative to the $\hat{\mathbf{x}}$ measurement. Because τ_η and θ_η are additional irrelevant unknowns, we remove them from the analysis by solving for the relevant variables, τ and θ, obtaining

$$-i(\Omega\tau + \theta) = \ln\left[\frac{r_\eta \widetilde{E}_\eta(\Omega)e^{-i(\Omega\tau_\eta+\theta_\eta)} - \cos\eta\,\widetilde{E}_x(\Omega)}{r\sin\eta\,\widetilde{E}_y(\Omega)}\right]. \tag{1}$$

The left side of this equation is purely imaginary. Taking the *real* part of the right side of Eq. (1) and expanding the logarithms in terms of $\ln[\widetilde{E}(\Omega)] = \ln|\widetilde{E}(\Omega)| - i\phi(\Omega)$, where $\phi(\Omega) = -\arg[\widetilde{E}(\Omega)]$ is the spectral phase, yields $\Omega\tau_\eta + \theta_\eta = \phi_x(\Omega) - \phi_\eta(\Omega) - \cos^{-1}[\Gamma(\Omega)]$, independent of τ and θ, where

$$\Gamma(\Omega) = \frac{r_\eta^2\,|\widetilde{E}_\eta(\Omega)|^2 + \cos^2\eta\,|\widetilde{E}_x(\Omega)|^2 - r^2\sin^2\eta\,|\widetilde{E}_y(\Omega)|^2}{2r_\eta\cos\eta\,|\widetilde{E}_\eta(\Omega)|^2|\widetilde{E}_x(\Omega)|^2}. \tag{2}$$

The equations in τ, θ and τ_η, θ_η are both in the form of a straight line with frequency Ω, and linear regression fits yield the slopes, τ and τ_η, and intercepts, θ

and θ_η. Thus, three measurements of the complex spectral field yield the complete time-varying polarization state.

This analytical approach can be used with any measurement technique that yields the pulse intensity and phase, such as FROG [14], SPIDER [15], or MIIPS [16]. In experiments, we found that the additional redundant information contained in FROG measurements provides more robust reconstructions via a simple fitting procedure. In this approach, the $\widetilde{E}_x(\Omega)$ and $\widetilde{E}_y(\Omega)$ fields are reconstructed [17]. FROG traces and amplitude ratios at angles η are simulated for different values of τ and θ, and the optimal values are searched by minimizing the error relative to the measured data.

We first measured two different elliptical polarizations, obtained by passing near-transform-limited, 90 fs pulses from a 1.55 μm Er-fiber laser (Precision Photonics, Boulder, Colo., USA) through a zero-order quarter-wave plate (Tower Optical, Boynton Beach, Fla., USA) at different angles relative to the $\hat{\mathbf{x}}$ axis. Four pulse projections (at $\eta = 0, 90°, \pm 45°$) were measured using a home-built second-harmonic generation (SHG) FROG, employing a 2.5 mm BBO crystal (EKSPLA, Vilnius, Lithuania) cut at 23.2°. Since a quarter-wave plate induces polarization ellipticity exclusively via amplitude division, the FROG traces for all projections are identical and power measurements are thus indispensable. From the measurements, the TURTLE algorithm retrieved power ratios $R \equiv r_{+45°}/r_{-45°} = 1.10$ and 1.43, which may be compared with the measured values of 1.12 and 1.63, respectively.

In the case of SHG-FROG, there are additional ambiguities in the retrieved signs of each spectral phase $\phi(\Omega)$. These translate to an ambiguity in the *relative* sign between the spectral phases of $\widetilde{E}_x(\Omega)$ and $\widetilde{E}_y(\Omega)$ and an *overall* ambiguity in the time axis, and therefore helicity, of the reconstructed pulse. These ambiguities are easily mitigated [18]. In our case, the TURTLE algorithm tried different combinations of field conjugations to get the best fit. Non-self-referenced techniques such as POLLIWOG and cross-FROG suffer from added difficulties due to the requisite interferometric stability between shaped and reference pulses. As with other self-referencing pulse characterization methods [14–16], the carrier-envelope offset phase [19,20] is not measured.

We used an amplitude-phase-polarization shaper described elsewhere [8] to obtain more complex arbitrary pulse shapes to be characterized by TURTLE. Figure 1 shows a measurement of a pulse obtained by delaying the polarizations by 50 fs relative to each other. "Phantom" traces, which compare measured (left half-plane) with reconstructed (right half) FROG traces, are shown for $\widetilde{E}_x(\Omega)$ and $\widetilde{E}_y(\Omega)$ in Figs. 1(a) and 1(b), respectively, together with the reconstructed pulse shape (horizontal), spectrum (vertical), and spectral phase (dashed). The relative delay between the polarizations is not revealed in the reconstructions. The measured (left half) and retrieved (right half) FROG traces for the $\pm 45°$ polarizations,
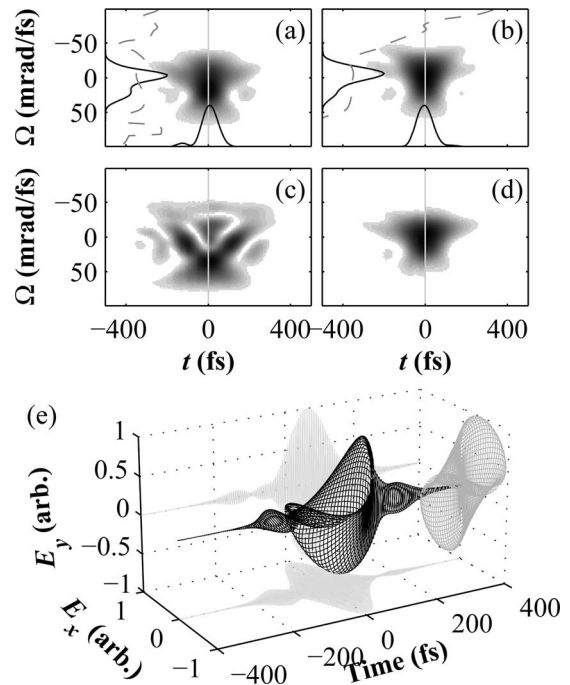

Fig. 1. Reconstruction of a pulse obtained by applying a 50 fs relative delay between the polarizations using a pulse shaper.

using the retrieved values of $\tau = 70.1$ fs and $\theta = 0.50$ rad, are shown in Figs. 1(c) and 1(d). The reconstructed field evolution is portrayed in Fig. 1(e) and yielded an amplitude ratio $R = 0.56$, which may be compared with the measured value of 0.80.

The discrepancy between applied and retrieved delays in Fig. 1 is attributed to incomplete delay compensation within the pulse shaper. Figure 2 shows the retrieved values of τ for a series of increasing delays applied using the shaper. The success with which the minimization algorithm retrieves the phase and delay depends on the topology of the error surface, an example of which is shown in the inset to Fig. 2. Due to the relative time-reversal ambiguity of $\widetilde{E}_x(\Omega)$ and $\widetilde{E}_y(\Omega)$, each measurement leads to two error surfaces and two retrieved delays. The error sur-
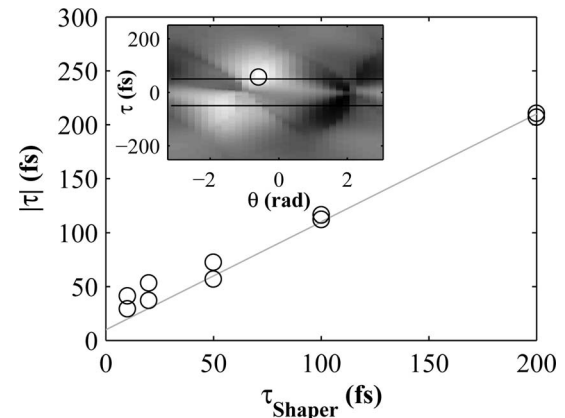

Fig. 2. Retrieved delays versus delays imposed using a pulse shaper. Inset, error surface as function of trial θ and τ values; light shades represent better fits. The black lines show the programmed delay in this case, and the circle the lowest point on the error surface.

faces were observed to be close to mirrored along the τ direction, with a corresponding sign flip in the retrieved delay τ. From Fig. 2, we find good agreement between imposed and retrieved delays, with a ~10 fs offset due to imperfect delay matching in the shaper.

Complicated pulse shapes, leading to highly structured FROG traces, can obviate the need for independent power measurements for determining the r coefficients. In Fig. 3, we show, analogously to Fig. 1, results for a simulation of 90 fs pulses with a sinusoidal spectral phase. The retrieved ±45° projections, obtained by a three-parameter search over τ, θ, and r, are shown in Figs. 3(c) and 3(d). The reconstructed field shown in Fig. 3(e) was qualitatively in excellent agreement with the simulated source field.

We have demonstrated self-referenced measurements of ultrafast laser pulses with both simple and nontrivial polarization states. The self-referenced pulse measurements are based on a set of at least three measurements of the complex pulse spectra projected along specific polarization directions. An analytic expression was found that extracts the full polarization state of an ultrafast laser pulse for this minimum set of complex spectral measurements. We found that a minimization procedure operating on two orthogonal and two interference FROG traces provides robust experimental extraction of the complete polarization state. The overconstraint of the FROG measurements likely contributes to the robustness of the polarization state retrieval. It should be noted that any complex spectral phase measurements will work with TURTLE.

Fig. 3. Simulated field reconstructions without supplied amplitude coefficients r. See text for details.

References

1. T. Brixner, G. Krampert, T. Pfeifer, R. Selle, G. Gerber, M. Wollenhaupt, O. Graefe, C. Horn, D. Liese, and T. Baumert, Phys. Rev. Lett. **92**, 208301 (2004).
2. T. Suzuki, S. Minemoto, T. Kanai, and H. Sakai, Phys. Rev. Lett. **92**, 133005 (2004).
3. M. Kakehata, R. Ueda, H. Takada, K. Torizuka, and M. Obara, Appl. Phys. B **70**, S207 (2000).
4. A. M. Weiner, Rev. Sci. Instrum. **71**, 1929 (2000).
5. S. M. Weber, F. Weise, M. Plewicki, and A. Lindinger, Appl. Opt. **46**, 5987 (2007).
6. M. Plewicki, F. Weise, S. M. Weber, and A. Lindinger, Appl. Opt. **45**, 8354 (2006).
7. D. Oron, N. Dudovich, and Y. Silberberg, Phys. Rev. Lett. **90**, 213902 (2003).
8. O. Masihzadeh, P. Schlup, and R. A. Bartels, Opt. Express **15**, 18025 (2007).
9. C. G. Slater, D. E. Leaird, and A. M. Weiner, Appl. Opt. **45**, 4858 (2006).
10. W. J. Walecki, D. N. Fittinghoff, A. L. Smirl, and R. Trebino, Opt. Lett. **22**, 81 (1997).
11. B. Haase, Opt. Lett. **24**, 543 (1999).
12. J. J. Ferreire, R. de la Fuente, and E. López-Lago, Opt. Lett. **26**, 1025 (2001).
13. M. Born and E. Wolf, *Principles of Optics*, 7th ed. (Cambridge U. Press, 1999).
14. R. Trebino and D. J. Kane, J. Opt. Soc. Am. A **10**, 1101 (1993).
15. C. Iaconis and I. A. Walmlsely, Opt. Lett. **23**, 792 (1998).
16. V. V. Lozovoy, I. Pastirk, and M. Dantus, Opt. Lett. **29**, 775 (2004).
17. D. Kane, IEEE J. Sel. Top. Quantum Electron. **4**, 278 (1998).
18. R. Trebino, *Frequency-Resolved Optical Gating: The Measurement of Ultrashort Laser Pulses* (Kluwer, 2000).
19. J. Reichert, R. Holzwarth, T. Udem, and T. W. Hänsch, Opt. Commun. **172**, 59 (1999).
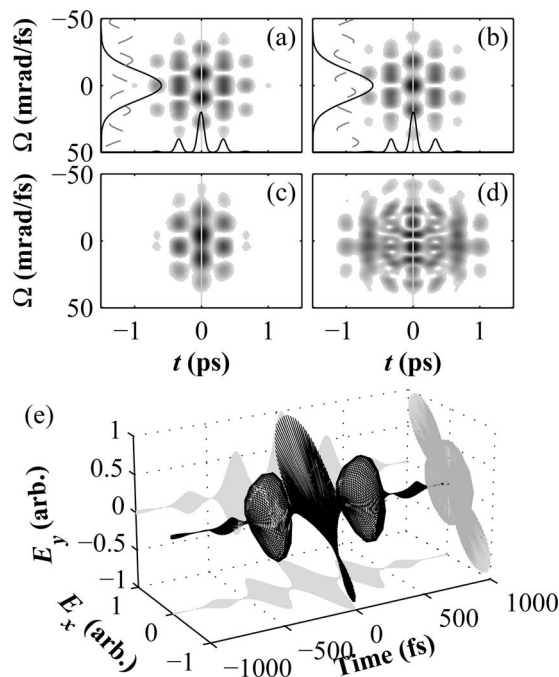20. H. R. Telle, G. Steinmeyer, A. E. Dunlop, J. Stenger, D. H. Sutter, and U. Keller, Appl. Phys. B **69**, 327 (1999).